

## PREDICTING LOCALIZED CO<sub>2</sub> CORROSION IN CARBON STEEL PIPELINES

Hui Li

Institute for Corrosion and Multiphase Technology  
Department of Chemical & Biomolecular Engineering  
Ohio University  
342 West State Street  
Athens, OH 45701

Bruce Brown

Institute for Corrosion and Multiphase Technology  
Department of Chemical & Biomolecular Engineering  
Ohio University  
342 West State Street  
Athens, OH 45701

Srdjan Nešić<sup>(1)</sup>

Institute for Corrosion and Multiphase Technology  
Department of Chemical & Biomolecular Engineering  
Ohio University  
342 West State Street  
Athens, OH 45701

### ABSTRACT

A mechanistic model is being developed with the aim of predicting localized CO<sub>2</sub> corrosion in carbon steel pipelines. The model is built based on a galvanic coupling mechanism proposed to be responsible for pit propagation of carbon steel in a CO<sub>2</sub> environment. Various phenomena associated with the localized corrosion process, such as electrochemical reactions, chemical reactions, mass transfer, FeCO<sub>3</sub> film formation, passivation, depassivation and repassivation are taken into account in the model to generate a complete and realistic simulation of field conditions.

Both uniform and localized corrosion rates can be predicted depending on how corrosion conditions evolve with time. The model calculates the change of corrosion condition at each time step to determine if a uniform or localized corrosion model should be used. In addition, this model provides users with other valuable information, such as local water chemistry, fluxes of species, and film morphology to help users understand the corrosion process. A parametrical study shows the effect of a variety of factors on the corrosion process which is in agreement with common knowledge about localized corrosion.

**KEY WORDS:** mechanistic model, galvanic, corrosion prediction, CO<sub>2</sub> corrosion, localized corrosion

---

<sup>(1)</sup> Corresponding author, E-mail address: nesic@ohio.edu (S. Nestic).

# INTRODUCTION

Localized corrosion is considered one of the most destructive forms of corrosion in the oil and gas industry. Although normally occurs over a limited surface area, it can lead to failure of pipelines and equipment in a relatively short period of time due to its high propagation rate. Consequently, localized corrosion is a major concern in the oil and gas industry as its normal operation is heavily dependent on the integrity of low cost carbon steel pipelines, normally passing over thousands of miles over land, underground and subsea. Significant efforts have been made towards understanding corrosion mechanisms over the past few decades. Today, researchers have reached a sufficient level of knowledge that enables them to propose theoretically sound mechanisms for uniform corrosion of carbon steel which are supported by empirical data.<sup>1</sup> Except for a few minor aspects, uniform corrosion of carbon steel can be said to be well understood. However, what happens in localized corrosion for carbon steel remains far less clear. Despite extensive past research, the mechanistic understanding of localized corrosion remains far from adequate. This is partly because water chemistry, particularly surface water chemistry, in the very small area of a pit is normally inaccessible by conventional equipment and differs substantially from the bulk solution. The complexity of localized corrosion is aggravated by the fact that initiation of pitting corrosion appears to be a (semi) random process in terms of when and where pits happen. Intuitively, one can say that pit initiation is also associated with the physical and chemical environment in close proximity to the metal surface. Therefore, it is critical to find a way to determine conditions near the steel surface, such as water chemistry and electrochemical phenomena, in order to understand what happens in localized corrosion. Unfortunately, up to now, few experimental methods have been found that can reliably detect localized corrosion or local water chemistry<sup>2</sup>, making it one of the biggest challenges for corrosion research. Therefore, a mechanistic model can be helpful in assisting the understanding of localized corrosion of carbon steel.

The goal of this paper is to present a transient mechanistic model that can be used to predict the details of the corrosion process of mild steel exposed to the CO<sub>2</sub> environment. The model is built based upon fundamental theories governing chemistry, electrochemistry and transport phenomena. The evolution of the corrosion process is simulated as a function of time. Depending on specific physical and chemical conditions, uniform or localized corrosion might be experienced. After a randomized event is used for the initiation step of localized corrosion, the model can predict and simulate the transition from uniform to localized corrosion according to appropriate theories. Various factors affecting corrosion processes, such as FeCO<sub>3</sub> film precipitation and dissolution, solution resistance, passivation, depassivation and repassivation are built into the model to give a comprehensive and physically realistic description of the actual process. Other than the corrosion rate, the model also provides users with valuable information which can help evaluate the environment and explain the corrosion behavior including: electrochemical potential, concentrations of species, fluxes of species, FeCO<sub>3</sub> film properties at any given location and time. It is not the intention of this paper to demonstrate the agreement between the model and the experimental data. Instead, the emphasis is placed on how the major theories used in this model describe the interaction of the key physical and chemical parameters with time. A more detailed model calibration and validation will be reported at a later stage.

In the following sections, the various processes simulated in the model are qualitatively described, followed by theories governing various phenomena and mathematical description of the theories. The model results are then presented to enable discussion of what happens in the localized corrosion process. The assumptions and limitations of the model are presented in the later portion of the paper.

## PHYSICOCHEMICAL PROCESSES DESCRIBED BY THE MODEL

It is generally agreed that there are three important stages in the localized corrosion process governed by a galvanic coupling mechanism: passivation/depasivation of the steel surface, pit initiation and pit propagation. Each of these processes has its unique mechanism and characteristics and therefore has to be treated separately. The processes simulated in this model are described below.

When a piece of metal is in contact with the solution, electrochemical reactions occur on the metal surface. Some species are consumed and others are generated, therefore concentration gradients of the species are established. As the corrosion process proceeds, ferrous ion ( $\text{Fe}^{2+}$ ) is continuously released into the solution; this varies the water chemistry. When the product of the concentrations for  $\text{Fe}^{2+}$  and  $\text{CO}_3^{2-}$  in the solution exceeds the solubility limit of  $\text{FeCO}_3$ , it will precipitate out of the solution and build a layer on the metal surface. This deposited corrosion product poses a significant mass transfer resistance to corrosive species (including  $\text{H}^+$ ) moving to/ from the bulk solution which leads to an increased pH at the metal surface. The pH increase provides a possibility for the formation of a pseudo-passive phase between and beneath corrosion product layer, thought to be a mixture of  $\text{FeCO}_3$ ,  $\text{Fe}(\text{OH})_2$  and/or  $\text{Fe}_3\text{O}_4$ .<sup>3</sup> As a result of passivation, the potential of the metal increases<sup>3</sup>. Up to this point in the description, the metal is experiencing uniform corrosion. It can be assumed that at some point in time, a small area of the metal loses its protective film leading to depassivation and consequent potential drop in this area. Therefore, a potential difference between this small film-free actively corroding area (which has now become an anode) and the large film-covered passive area around it (which has now become a cathode) is established. This potential difference serves as the driving force for galvanic pit propagation<sup>4</sup>. In a specific case in which supersaturation of  $\text{FeCO}_3$  in the solution is sufficiently high, the substantial amount of  $\text{Fe}^{2+}$  resulting from pit propagation will promote further precipitation of  $\text{FeCO}_3$  on the anode. This will increase the surface pH of the anode and facilitate repassivation, eventually leading to pit repassivation (“pit death”). The processes described above are schematically illustrated in Figure 1.

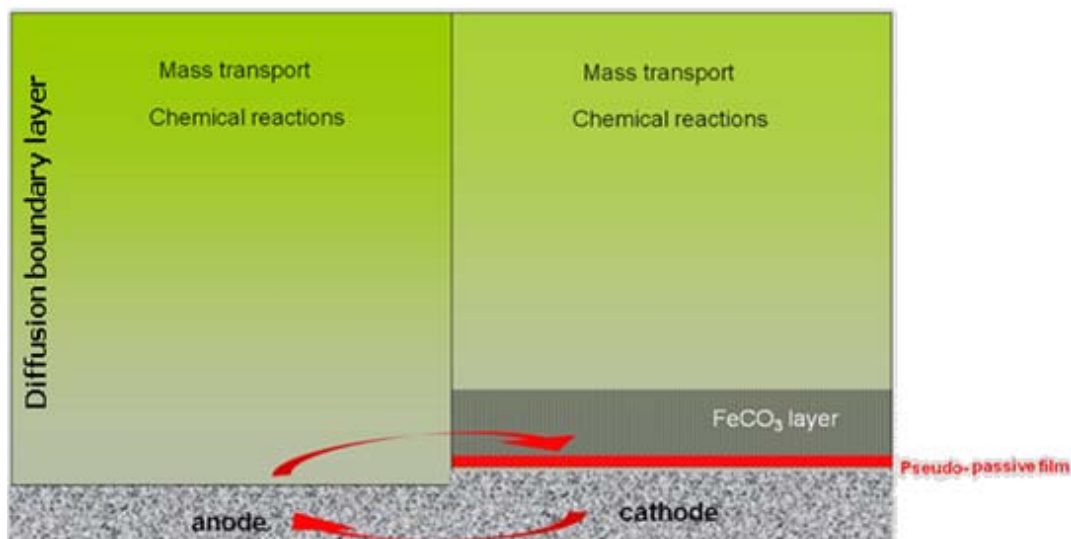


Figure 1: Schematic illustration of the computational domain used in the model: steel surface with a partially removed  $\text{FeCO}_3$  layer on the anode.

## THEORY BEHIND THE MODEL

Various phenomena occurring simultaneously in the corrosion process are governed by a few fundamental laws of physical chemistry. The main theories used in the model are presented in this section.

### Mass Transport

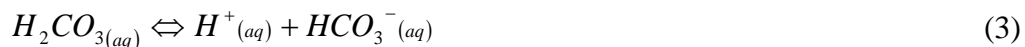
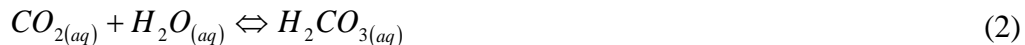
Mass transport is an important process since it determines concentration gradient in the boundary layer near the steel surface, and therefore alters electrochemical reaction kinetics. Mass transport of species is mainly affected by three mechanisms: molecular diffusion, electromigration, and convection.

Convection is typically the biggest contributor to mass transport as turbulent eddies can penetrate deep into the diffusion layer and shorten the distance over which diffusion and electromigration take place. However, convection plays a small role when significant  $\text{FeCO}_3$  film forms on the steel surface and presents a significant diffusion barrier.

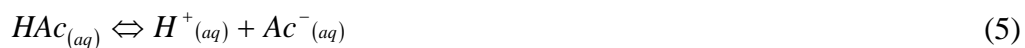
### Chemical Reactions

It is generally agreed that most chemical reactions proceed much faster than other processes involved in corrosion, such as mass transport and electrochemical reactions. Therefore, many corrosion models neglect the chemical reaction effect on mass transport by assuming that chemical equilibrium is preserved in the solution. This assumption would fail in a  $\text{CO}_2$  corrosion environment since  $\text{CO}_2$  hydration, reaction (2), was found to be a slow step<sup>5</sup> and in some cases becomes a rate limiting step in the  $\text{CO}_2$  corrosion process. Hence, a local non-equilibrium condition is likely to exist which makes the chemical reaction rate an important factor in  $\text{CO}_2$  corrosion.

For a  $\text{CO}_2$  system, the following reactions are considered to always exist:



Of course, the above mentioned reactions are not the only possibilities in a real system since many other species could be present in field brine. For example, when acetic acid,  $\text{CH}_3\text{COOH}$  (shortly: HAc) is found in water, its dissociation has to be taken into account as it can become a major source for providing  $\text{H}^+$ :



Another important chemical reaction that plays a vital role in  $\text{CO}_2$  corrosion is  $\text{FeCO}_3$  precipitation, reaction (6). It was already argued that the  $\text{FeCO}_3$  layer, once formed, often controls the rate of

corrosion<sup>1</sup>. FeCO<sub>3</sub> affects corrosion process in three distinct ways. First, as FeCO<sub>3</sub> is formed by precipitation, it acts as the sink for Fe<sup>2+</sup> and CO<sub>3</sub><sup>2-</sup> ions altering their concentrations in the solution and leading to local acidification of the solution. Second, the tortuous path through the discontinuous FeCO<sub>3</sub> layer poses a significant mass transfer resistance to species moving towards or away from the metal which slows down the electrochemical reactions. Third, the presence of FeCO<sub>3</sub> film on the metal surface effectively reduces the surface area exposed to the corrosive environment by covering up parts of the surface.



Unlike other chemical reactions occurring homogeneously in the solution, FeCO<sub>3</sub> precipitation is a heterogeneous process. Nucleation of solid iron carbonate occurs preferentially on the steel surface or inside the void space within the present solid layer.<sup>6</sup>

For the localized corrosion process, Fe<sup>2+</sup> hydrolysis is considered to be an important reaction which will promote passivation of the metal surface, an essential step in forming a galvanic cell. This reaction will be discussed in more details below.

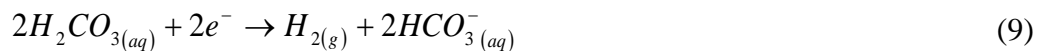
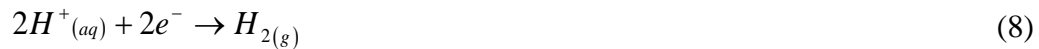
A more complete list of possible chemical reactions occurring in field brine found in oil and gas pipelines and associated rate constants can be found elsewhere.<sup>1</sup>

### Electrochemical Reactions

In a typical CO<sub>2</sub> corrosion environment, a number of electrochemical reactions can occur simultaneously. The dominant anodic reaction is iron dissolution as shown by reaction (7). As previously argued<sup>1</sup>, even though this reaction has been reported to be dependent on pH and CO<sub>2</sub> partial pressure, the effect of these parameters tends to rapidly diminish when pH>4, which is a typical environment in an oil and gas pipelines containing CO<sub>2</sub>. Therefore, the dependence of anodic dissolution rate on pH and CO<sub>2</sub> is neglected in the model.



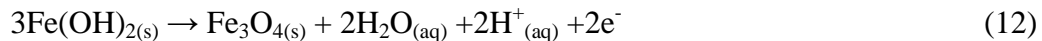
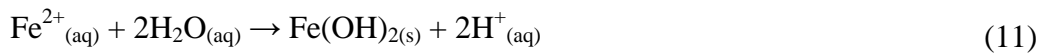
The cathodic reactions considered in the model include H<sup>+</sup> reduction, H<sub>2</sub>CO<sub>3</sub> direct reduction and HAc direct reduction, as shown by reactions (8), (9) and (10) respectively. Water reduction is not taken into account as in a typical CO<sub>2</sub> environment, contribution of this reaction to the overall reaction rate would be negligible.<sup>1</sup>



A detailed description of electrochemical reactions listed above can be found in the open literature for  $CO_2$  corrosion<sup>7</sup> and will not be discussed here.

## Passivation

The research carried out in the past few years has revealed the galvanic coupling mechanism of localized corrosion for carbon steel in  $CO_2$  environments<sup>4</sup>. It was observed that under proper conditions, carbon steel exhibited a substantial increase in potential suggesting the occurrence of passivation on steel surface. Steel surface analysis confirmed the existence of magnetite ( $Fe_3O_4$ ) and/or  $Fe(OH)_2$ , species commonly known to be related to passivity.<sup>3</sup> Passivation of a metal can be a precursor to the occurrence of localized corrosion as passivation can significantly raise the potential of the metal substrate and create a substantial potential difference once depassivation occurs in other areas. In this model, magnetite formation is proposed to form via a two-step process as shown in equation (11) and (12). In this process, the formation of  $Fe(OH)_2$  resulting from  $Fe^{2+}$  hydrolysis and subsequent oxidation of  $Fe(OH)_2$  to form magnetite.



Passivation has been said to be a fast process compared to other reactions in the corrosion process<sup>2</sup>; therefore, the kinetics of this reaction are not considered important. In this model, passivation is considered to be governed solely by thermodynamic conditions associated with formation of magnetite. This is to say, once thermodynamic conditions become favorable for the formation of magnetite through reactions (11) and (12), passivation is considered to occur immediately.

Cathodic current density on passive surface. Upon passivation, the carbon steel surface is covered by a thin but dense and protective oxide layer. Unlike an active carbon steel surface, the passive film is electrically semi-conductive. It is well known that anodic passive current density is attributed to the semi-conductivity of passive film; however, how the semi-conductive passive film influences the kinetics of cathodic reactions is also an important topic in the modeling practice. In this work, an effort has been made to compare the cathodic reaction rate on passive and active steel surfaces. A direct comparison for cathodic reaction kinetics between passivated and active carbon steel cannot be easily achieved by commonly used electrochemical techniques (such as potentiodynamic sweep). This is because corrosion of carbon steel in a  $CO_2$  environment is normally under mixed charge transfer/chemical reaction limiting control, which makes it difficult to obtain information about the charge transfer reaction. The significant difference in open circuit potential of active and passivated carbon steel further prohibits the direct comparison of cathodic reactions. An example of potentiodynamic sweeps for stainless steel (a surrogate passive surface) and carbon steel (an active surface) is schematically shown in Figure 2. While it is hard to derive a general conclusion related to the similarity/dissimilarity of cathodic reaction rate for passivated and active steel surfaces due to the large difference in the open circuit potential of the two steels, one can at least conclude that the limiting current is the same. A different strategy was adopted to fill in the missing information about the charge transfer kinetics of this reaction on the two different surfaces. A simulation was run using FREECORP<sup>(†)</sup>, a software that is capable of generating the Evans diagram of the system in which the

---

<sup>(†)</sup> a freely available product of the Institute for Corrosion and Multiphase Technology, Ohio University distributed under the GNU General Public License.

relation between potential and current density for electrochemical reactions can be shown. By comparing the experimentally obtained potentiodynamic sweep for stainless steel with the total cathodic polarization curve generated from the software for carbon steel under the same conditions, as shown in Figure 3, it is evident that no significant difference exists between cathodic reaction rates on both stainless steel and carbon steel surfaces, which means the cathodic reaction rate is not heavily affected by the state of metal surface. This was also observed in a previous study which showed similar cathodic reaction kinetics on both carbon steel and Alloy 625 surface<sup>8</sup>. Therefore, it can be deduced that the passive film formed on carbon steel would not significantly change the cathodic reaction kinetics. For all practical purposes, the cathodic reaction rate on a passive surface can be treated as being the same for an active surface.

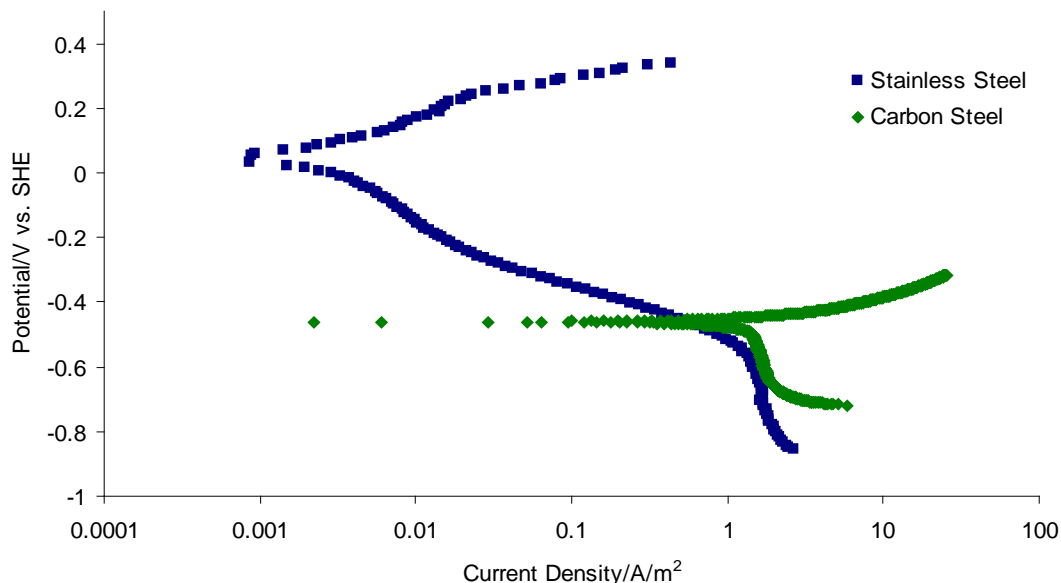


Figure 2: Potentiodynamic sweep on stainless steel and carbon steel. Test condition:  $T=25^{\circ}\text{C}$ ,  $\text{pH}=4.1$ ,  $\text{pCO}_2=1$  bar, stagnant solution

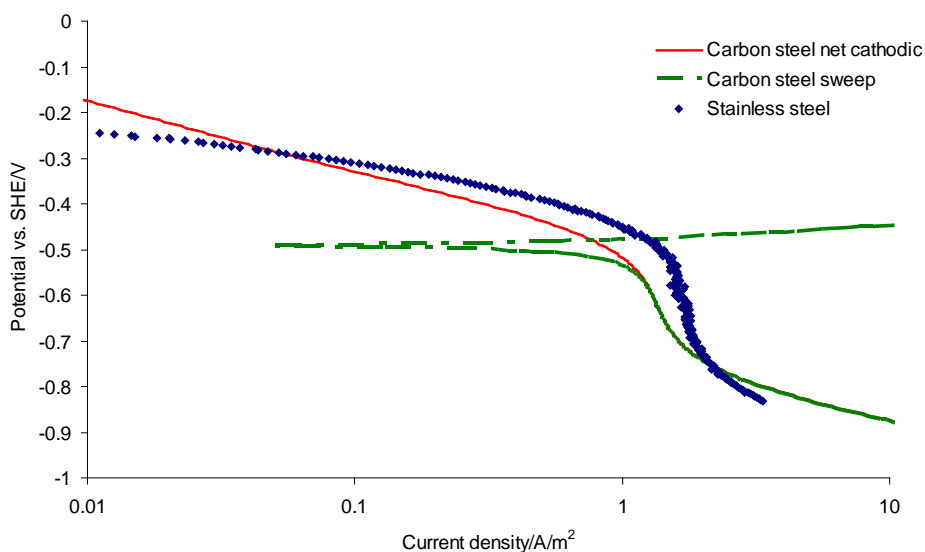


Figure 3: Comparison of potentiodynamic sweep of stainless steel with polarization curves of carbon steel generated from the software. Test conditions:  $T=25^{\circ}\text{C}$ ,  $\text{pH}=4$ ,  $\text{NaCl}=1\%$ , stagnant solution.

Anodic current density on passive surface. It has been suggested that pH, temperature and halide concentration are three parameters that play major roles in determining the passive current density. However, the experiments performed in this work do not support the effect of halide on passive current density of carbon steel in a CO<sub>2</sub> environment. Instead, pH, temperature and potential have been found to be the major factors. There is still an ongoing research effort focused towards finding the passive current densities at different pH, temperatures and potentials, which will be reported in the future.

### **Pit initiation**

Pit initiation is caused by a loss of passive layer on parts of the steel surface. In this model, pit initiation is considered to occur when FeCO<sub>3</sub> film is removed by mechanical or chemical forces, which results in destruction of the passive film and exposure of the active surface to H<sup>+</sup>, Cl<sup>-</sup>, and/or other aggressive species. The exact mechanism of FeCO<sub>3</sub> film removal is still under investigation, however, experimental observations seem to suggest that pit initiation occurs randomly in terms of when and where it is going to happen. In order to mimic the stochastic nature of pit initiation, a random function needed to be incorporated into the model. In this model, the Weibull distribution random function was used. H. Ascher<sup>9</sup> defined the initiation time for each of the pits on a coupon as the time at which first failure of the system occurs. Following his reasoning, the Weibull distribution is a good candidate for simulating pit initiation as it is the most widely used function in failure analysis. For example, a DNV standard describes a method to determine probability of failure based on the Weibull distribution.<sup>10</sup> One of the unique advantages of using a Weibull distribution is that, depending on the parameters provided, this function can take different shapes of other commonly used functions such as normal, lognormal, etc. This provides a flexibility of controlling how pit initiation behaves with respect to time.

### **Pit propagation**

Pit propagation attracts the most attention from corrosion engineers. Once initiated, a pit can quickly penetrate into the metal at a high rate. On the other hand, some pits, once initiated, can propagate for a short time and then stop (pit “death”). The rate of pit propagation directly affects the lifetime of pipelines and facilities. Different strategies and assumptions have been employed in various models in accordance with specific materials and corrosive environments. For carbon steel corroded in a CO<sub>2</sub> environment, the galvanic coupling mechanism was found to govern pit propagation<sup>4</sup>. Once local depassivation happens on a small area, a potential difference is established between this active surface (anode) and the passive surface around it (cathode). This proceeds so that the cathodic current occurring on a large area cathode is balanced by the anodic current on a small area anode, leading to a substantial anodic dissolution rate.

However, the potential difference between anode and cathode would generate an unrealistically high pit propagation rate (10<sup>2</sup> mm/y or higher) that is not observed in reality. Pickering *et al*<sup>11</sup> proposed an IR potential drop mechanism (solution resistance between electrodes) that can offer an explanation. In a uniform corrosion scenario, anode and cathode are so close to each other that solution resistance does not play a vital role as long as some supporting electrolyte is present. However, in the case of localized corrosion, separation of anode and cathode is experienced leading to significant solution resistance between anode and cathode. This solution resistance can significantly limit the anodic dissolution rate. Depending on how far the anode is from the cathode, the pit propagation rate would be different as solution resistance varies with the distance between electrodes. Obviously, neglecting the effect of solution resistance would lead to over-prediction of the pitting corrosion rate.

## Repassivation

Repassivation is a process in which an active steel surface regains passivity under proper conditions leading to suspension of pit propagation. It is proposed in this model that in a CO<sub>2</sub> environment, repassivation occurs when solution supersaturation with respect to FeCO<sub>3</sub> becomes sufficiently high, which would trigger fast precipitation of FeCO<sub>3</sub> inside the pit. This would raise surface pH to a level at which passive film formation is favorable. At the same time, increased Fe<sup>2+</sup> concentration also helps drop the critical pH required for the formation of Fe(OH)<sub>2</sub>. As can be seen in equation (26), this further favors repassivation. In this model, repassivation is determined by the same thermodynamic criterion as used for passivation.

## MATHEMATICAL DESCRIPTION OF THE MODEL

The processes presented in the previous section can be mathematically described by equations describing mass transport, electrochemical reactions, solution resistance, FeCO<sub>3</sub> film growth, etc.

### Mass Transport

Mass transport of species in a dilute system is governed by the law of mass conservation, the so called Fick's second law. In the presence of porous film, the equation has to be modified to take into account characteristics (e.g. porosity and tortuosity) of the film<sup>12</sup>:

$$\frac{\partial \varepsilon c_j}{\partial t} = -\nabla \cdot \kappa N_j + \varepsilon R_j \quad (13)$$

Where  $c_j$  is the concentration of species,  $\varepsilon$  is the porosity of FeCO<sub>3</sub> film,  $\kappa$  is permeability of FeCO<sub>3</sub> film which is defined as the product of porosity ( $\varepsilon$ ) and tortuosity ( $\xi$ ) of the film;  $t$  is time;  $N_j$  is the flux of species and  $R_j$  is chemical reaction rate of species.

The first term on the RHS of equation (13), flux of species, is given by:

$$N_j = -D_j \nabla c_j - z_j u_j F c_j \nabla \phi + c_j v \quad (14)$$

Where  $D_j$  is the diffusion coefficient;  $z_j$  is the electrical charge;  $\phi$  is the electrostatic potential in the solution;  $F$  is the faraday constant;  $v$  is the in-situ flow velocity and  $u_j$  is the mobility of species which can be calculated as:

$$u_j = \frac{D_j}{RT} \quad (15)$$

Where  $R$  is universal gas constant and  $T$  is temperature.

It can be seen that the flux of species is attributed to three components which take into account the contributions from molecular diffusion, electro-migration and convection, respectively. The convection term requires the knowledge of in-situ velocity, which would typically require the solution of the

Navier-Stokes equations. This process would be time consuming as computational flow dynamics itself is an independent and complicating subject. To expedite the calculation, Nesic, *et al.*<sup>1</sup> have suggested that for this purpose a way to approximate the convection effect is by using a so-called ‘turbulent diffusivity’ in the computation domain. Within the solid film, it is assumed that flow dissipates and species can travel through the film only by molecular diffusion and electromigration.

The flux due to electromigration can be usually neglected in the case of uniform corrosion. The potential gradient generated by different diffusion rates of species is often easily annihilated by large amounts of supporting species, such as Na<sup>+</sup> and Cl<sup>-</sup>. However, neglecting the electromigration effect is unacceptable in localized corrosion case because of the significant potential difference between anode and cathode which could drive charged species to travel at appreciably different rates.

The second term on the RHS of equation (13) accounts for chemical reaction rates of species. Various species are coupled together through reactions shown in equation (1) to (5); therefore, mass transport equations for various species have to be solved simultaneously. The mathematical technique for dealing with chemical reaction rate was previously presented by Nesic, *et al.*<sup>1</sup> and will not be described here.

Calculation of mass transport is carried out in a pre-defined domain, the height of which equals the thickness of diffusion boundary layer. The thickness of diffusion boundary layer is given by<sup>13</sup>:

$$\delta = 25 \text{Re}^{-7/8} d \quad (16)$$

Where  $\delta$  is the thickness of diffusion boundary layer, Re is the Reynolds number and d is the hydraulic diameter.

The length of the computational domain (Figure 1) covers the metal surface with the anode placed on the left side of the steel surface at the bottom. Due to the significant time required to simultaneously solve the transient mass transport equations for all species involved in the corrosion process in a 2D domain, a simplification was made to achieve a compromise between accuracy and efficiency. Instead of a 2D domain, mass transport equations are solved in two 1D domains, for the anode and the cathode separately; anode and cathode are then coupled together for calculation of potential distribution which is distributed in a 2D domain. This simplification is probably acceptable, as mass transport takes place primarily in the direction perpendicular to metal surface, concentration gradient in the direction parallel to the metal surface is small and therefore would not significantly affect the electrochemical reaction rate on metal surface.

Outside the diffusion boundary layer, all species are well mixed by turbulent flow; therefore, little concentration gradient could be expected. For this reason, the boundary condition for the upper end of the computation domain is taken as the bulk concentrations of species. The fluxes of species are used to specify the boundary condition at metal surface. For species not involved in electrochemical reactions, zero flux is used, for corrosion-related species, e.g. H<sup>+</sup>, H<sub>2</sub>CO<sub>3</sub>, Fe<sup>2+</sup>, etc., flux can be obtained from electrochemical reaction rate by the following equation:

$$N_j = \frac{i_j}{z_j F} \quad (17)$$

Where  $i_j$  is the electrochemical reaction rate, which is dependent on surface concentration of corrosive species and metal surface potential.

In the model, initial condition for mass transport equations is taken to be the concentrations with which chemical equilibrium is satisfied.

### Film growth

The equation governing  $\text{FeCO}_3$  film growth was previously developed by Nescic and Lee<sup>14</sup> based on mass conservation of  $\text{FeCO}_3$  in the solution, as shown in equation (18). More detailed information about this equation can be found in the original paper.

$$\frac{\partial \varepsilon}{\partial t} = -\frac{M_{\text{FeCO}_3(S)}}{\rho_{\text{FeCO}_3(S)}} R_{\text{FeCO}_3(S)} - CR \frac{\partial \varepsilon}{\partial x} \quad (18)$$

Where  $M_{\text{FeCO}_3(S)}$  and  $\rho_{\text{FeCO}_3(S)}$  are the molar mass and density of  $\text{FeCO}_3$ , respectively, CR is the corrosion rate,  $\varepsilon$  is the porosity of  $\text{FeCO}_3$  film,  $t$  and  $x$  are the coordinates in time and space.

### Solution potential distribution

In an electrochemical system, potential distribution happens on a much shorter time scale than mass transfer. It has been estimated that the time required to electrically neutralize an electrolyte is  $10^{-8}$  seconds<sup>15</sup>. This is described by the electrostatic potential distribution in the solution which is governed by Poisson's equation:

$$\nabla^2 \phi = -\frac{F}{\xi} \sum_j z_j c_j \quad (19)$$

where  $\xi$  is the permittivity of the electrolyte. For water, the quotient of  $F/\xi$  is very large, which physically indicates that any small separation of charge would generate a significant potential gradient which tends to rapidly restore the system to the state of electroneutrality. The strong force resulting from a large electrostatic potential gradient can annihilate any charge imbalance at a speed much faster than that of mass transport. Because potential distribution happens on a much shorter time scale, it is commonly assumed that electroneutrality is always obeyed at any point in time. Therefore, equation (19) can be safely replaced with the following equation without introducing significant errors:

$$\nabla \cdot (\sigma \nabla \phi) = 0 \quad (20)$$

where  $\sigma$  is the conductivity of the electrolyte. Clearly, equation (20) assumes an environment where electroneutrality is satisfied everywhere and at all times in the solution.

Unlike the mass transport process where a 1D domain is sufficient, significant potential gradient can be present not only in the direction parallel to the metal surface, but also perpendicular to the metal surface. This is particularly true for the localized corrosion processes since charged species (currents) flow through the solution in both directions due to separation of the anode and the cathode. Therefore, it is

essential to calculate the potential distribution in a 2D domain (such as the one in Figure 4), height of which equals to the thickness of the liquid layer.

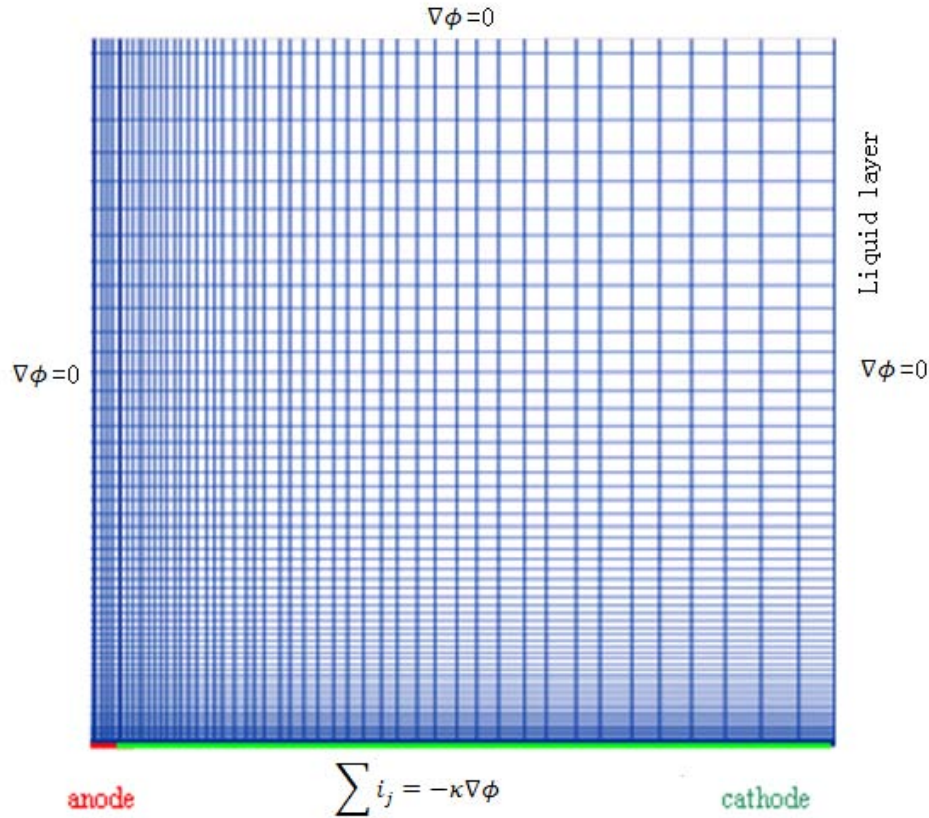


Figure 4: Computation domain and boundary conditions for the PDE equation for electrostatic potential in the solution.

The boundary condition for the steel surface is given by Kirchhoff's law,

$$\sum i_j = -\kappa\nabla\phi \quad (21)$$

Where  $i_j$  is the current density of individual electrochemical reactions on the metal surface.

For other boundaries (left, right and upper wall of computation domain), normal current density are set to zero as the right wall is far away from the metal surface and charged species would not be able to get to the boundaries, the upper wall defines the location where liquid phase (and therefore charged species) ends, while the left boundary maintains zero current density due to symmetrical configuration.

### Passivation/ repassivation

Passivation of carbon steel is determined based on thermodynamic conditions. A two-step process has been proposed to generate magnetite, the material responsible for passivation, as shown in equation (11) to (12). The Gibbs free energy was calculated for all species involved in the reactions using the following equation:

$$\Delta G(T) = \Delta H(T) - T \cdot \Delta S(T) \quad (22)$$

With the Gibbs free energy defined, the reversible potential for electrochemical reactions (equation (12)) or chemical equilibrium constant for chemical reactions (equation (11)) can be easily obtained with the following equations:

$$\Delta G^o = -nFE_{rev}^o \quad (23)$$

$$\Delta G^o = -RT \ln K_{eq} \quad (24)$$

The following equations are then used to determine the equilibrium potential and pH at which a passive film would be formed by taking into account the effect of concentrations of species:

$$E_{rev} = E_{rev}^o - \frac{RT}{nF} \ln \frac{a_{red}}{a_{ox}} \quad (25)$$

$$K_{eq} = \frac{a_{H^+}^2}{a_{Fe^{2+}}} \quad (26)$$

Where  $T$  is temperature,  $G$ ,  $H$  and  $S$  are the Gibbs free energy, enthalpy and entropy, respectively,  $n$  is number of moles of electrons involved in the electrochemical reactions,  $E_{rev}$  and  $E_{rev}^o$  are the reversible potential for electrochemical reactions at real and standard conditions, respectively.  $K_{eq}$  is the equilibrium constant for chemical reactions, where  $a_{H^+}$  and  $a_{Fe^{2+}}$  are the activities of  $H^+$  and  $Fe^{2+}$ , respectively, which are estimated in the model by the corresponding concentrations.

### Pit initiation

A Weibull distribution function is used to simulate the stochastic behavior of pit initiation in terms of time. Since this localized corrosion model is a two-point model, meaning corrosion rate is calculated only for two points, namely an anode and a cathode, it is not intended to simulate the random behavior related to location of the pits.

A two-parameter Weibull distribution function is defined as:

$$We(x) = \frac{\beta}{\alpha} \left( \frac{x}{\alpha} \right)^{\beta-1} e^{-\left( \frac{x}{\alpha} \right)^\beta} \quad (27)$$

Where  $We$  is the Weibull function,  $x$  is the independent variable,  $\alpha$  is the scale parameter,  $\beta$  is the shape parameter.

The scale and shape parameters are related to mean and standard deviation of the distribution in the following fashion:

$$\mu = \alpha \Gamma\left(1 + \frac{1}{\beta}\right) \quad (28)$$

$$\sigma^2 = \alpha^2 \left[ \Gamma\left(1 + \frac{2}{\beta}\right) - \Gamma^2\left(1 + \frac{1}{\beta}\right) \right] \quad (29)$$

Where  $\mu$  is the mean value,  $\sigma$  is the standard deviation and  $\Gamma$  is the gamma function which is further defined as:

$$\Gamma(z+1) = \int_0^{\infty} t^z e^{-t} dt \quad (30)$$

Therefore, a scale parameter and a shape parameter can be calculated by solving equations (28) and (29) based on the values of mean and standard deviation.

Once scale and shape parameters are obtained, a Weibull distribution random number can be generated based on a uniform distribution random number normally given by the built-in function in most software-developing packages:

$$y = \alpha \cdot [-\ln(1-x)]^{\frac{1}{\beta}} \quad (31)$$

Where  $y$  is the Weibull distribution random number and  $x$  is the uniform distribution random number between 0 and 1.

In this report, a mean value of 2 hours after passivation and a standard deviation of 0.5 hours are used to generate the time for pit initiation. These values were arbitrarily set and can be easily changed according to experimental findings.

### **Pit propagation**

Pit propagation is driven by the potential difference between anode and cathode. The pit propagation rate is governed by the metal potential at the steel surface. Due to the galvanic effect, the metal potential is able to accelerate the corrosion rate for anode and decelerate the corrosion rate for cathode. Solution resistance between anode and cathode also plays an important role in determining the pit propagation rate.

The metal potential for uniform corrosion is calculated based on the fact that the current density of anodic reactions must be balanced by that of the cathodic reactions, while potential for localized corrosion is obtained by solving equation (20):

$$\sum_{anodic} i = \sum_{cathodic} i \quad (32)$$

where  $i$  is current density of anodic or cathodic reactions.

The anodic and cathodic current densities are calculated by the Butler-Volmer equation as:

$$anodic : i_a = \begin{cases} i_o \times \left( 10^{\frac{E-E_{rev}}{b_a}} - 10^{\frac{E_{rev}-E}{b_c}} \right) & \text{for active surface} \\ i_{pass} & \text{for passive surface} \end{cases} \quad (33)$$

$$cathodic : i_c = i_o \times \left( 10^{\frac{E-E_{rev}}{b_a}} - 10^{\frac{E_{rev}-E}{b_c}} \right) \quad (34)$$

Where  $i_o$  is the exchange current density,  $i_{pass}$  is the passive current density,  $E_{rev}$  is the reversible potential,  $b_a$ ,  $b_c$  are the Tafel slope for anodic and cathodic branches of an electrochemical reaction and  $E$  is the metal potential.

With the knowledge of metal potential, the anodic dissolution rate can be calculated by solving equation (33).

## RESULTS AND DISCUSSION

Some calculated results are presented in this section to investigate the variations of important electrochemical and chemical parameters in the course of pitting corrosion and how changes in these parameters affect the corrosion rate.

Figure 5 through Figure 10 illustrate results for a specific case: temperature 80°C, CO<sub>2</sub> partial pressure 0.52 bar, liquid velocity 0.4 m/s, pipe diameter 0.1m, bulk pH 6.6, bulk supersaturation of FeCO<sub>3</sub> 1.05, passive current density 0.05A/m<sup>2</sup>. Bulk concentrations of species with which chemical equilibrium is maintained are listed in TABLE 1.

Figure 5 illustrates the corrosion rate change on both anode and cathode as a function of time. It can be seen that corrosion rate starts at about 6.5mm/yr indicating a very corrosive environment. The high corrosion rate at the beginning is due to the sudden environment change at the initiation of the simulation. Soon after the process of corrosion starts and the electrochemical reactions occur, the concentration gradient are established; therefore, the mass transfer effect start playing a role in the kinetics of electrochemical reactions and this slows down the overall reaction rates. This behavior was captured by the model as indicated by a sharp drop of the corrosion rate at the beginning of the simulated process. Due to corrosion, Fe<sup>2+</sup> slowly accumulates on the metal surface, leading to increased supersaturation of FeCO<sub>3</sub> in the solution. FeCO<sub>3</sub> precipitation then takes place as time evolves. The presence of FeCO<sub>3</sub> film, as discussed before, reduces the corrosion rate by covering part of metal surface and by increasing mass transfer resistance. Increased mass transfer resistance to H<sup>+</sup> also leads to a higher surface pH as can be seen in Figure 6. At about 68 hours, a sharp decrease of corrosion rate occurs. This is because the surface pH reaches the critical pH at which magnetite is formed leading to passivation of the metal surface. Clearly, up to this point, both anode and cathode are corroding at the same rate, that is, uniform corrosion has been happening on the metal surface. At about 70 hours, the model is set to

trigger a “pit initiation” event which wipes off protective films on the surface of the anode, including  $\text{FeCO}_3$  and passive film, and exposes the bare anode surface to the corrosion environment. The potential difference is then established between the active anode and the surrounding passive cathode, which forms a galvanic cell to drive the pit propagation. The corrosion rate of the anode is increased to about 8mm/yr and maintained at this level in the rest of the simulation. Clearly, this case presents a pit propagation scenario.

**Table 1**  
**Initial Concentrations for Tested Case**

Species	Initial concentration/M
$\text{H}^+$	$2.51 \times 10^{-7}$
$\text{OH}^-$	$8.56 \times 10^{-7}$
$\text{CO}_2$	$7.24 \times 10^{-3}$
$\text{H}_2\text{CO}_3$	$1.87 \times 10^{-5}$
$\text{HCO}_3^-$	$1.32 \times 10^{-2}$
$\text{CO}_3^{2-}$	$5.08 \times 10^{-6}$
$\text{Fe}^{2+}$	$1.74 \times 10^{-6}$
$\text{Na}^+$	$1.32 \times 10^{-5}$
$\text{Cl}^-$	$2.90 \times 10^{-7}$

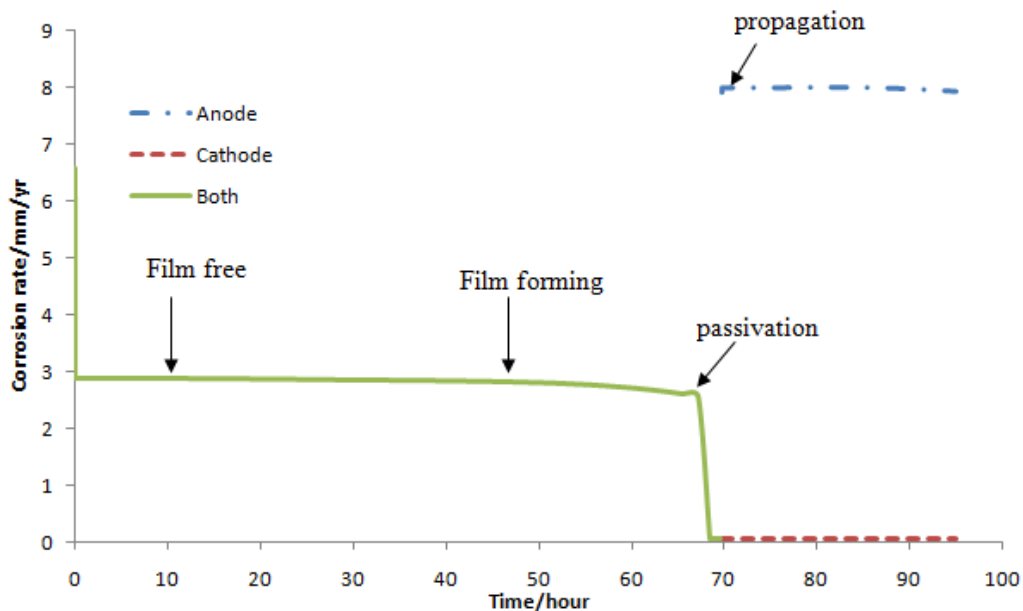


Figure 5: Corrosion rate change as a function of time. Simulation conditions: temperature 80°C,  $\text{CO}_2$  partial pressure 0.52bar, velocity 0.4m/s, pipe diameter 0.1m, bulk pH 6.6, bulk supersaturation of  $\text{FeCO}_3$  1.05, passive current density 0.05A/m<sup>2</sup>.

Figure 6 shows how surface pH varies as a function of time. It can be seen that surface pH starts at about 7, higher than the initial value of 6.6. This is due to the high corrosion rate which consumes a large quantity of  $H^+$ . Surface pH was then maintained at this value indicating a steady corrosion rate. At about 45 hours, surface pH begins to increase due to  $FeCO_3$  precipitation. The surface pH keeps increasing until it reaches about 7.05 at which the passive film is formed. As shown in Figure 5, passivation causes a significant drop of corrosion rate, a process consuming less  $H^+$  and leads to a lower surface pH. Initiation of pit at about 70 hours establishes a galvanic cell between anode and cathode, which results in a high propagation rate at the anode, this process releases much  $Fe^{2+}$  into the solution and increases surface pH, while a relatively low pH is maintained at the cathode where little corrosion is experienced. The pH value at the anode is maintained in the rest of the simulation, reflecting stable surface water chemistry and therefore stable corrosion rate.

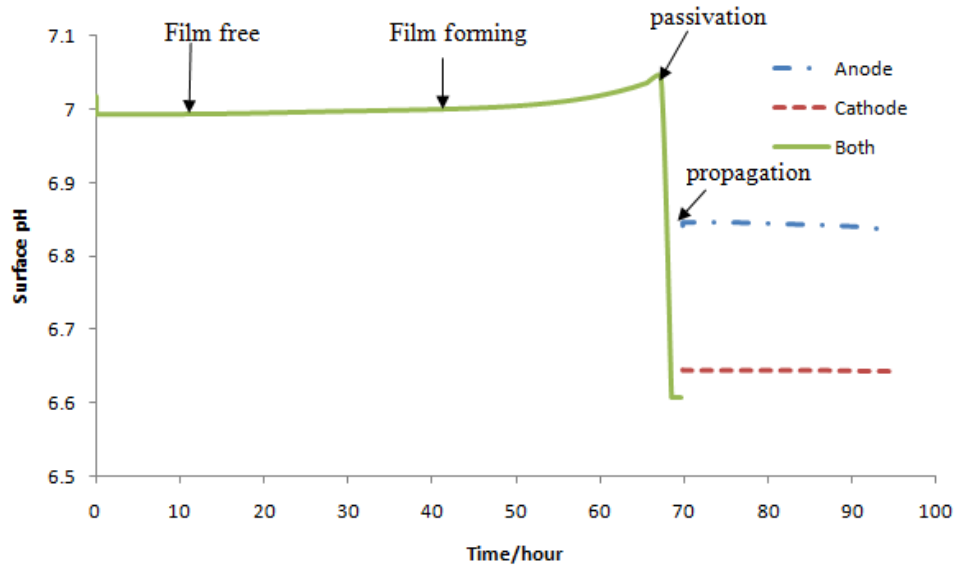


Figure 6: Surface pH variation as a function of time. Simulation conditions: temperature  $80^{\circ}C$ ,  $CO_2$  partial pressure 0.52bar, velocity 0.4m/s, pipe diameter 0.1m, bulk pH 6.6, bulk supersaturation of  $FeCO_3$  1.05, passive current density  $0.05A/m^2$ .

Figure 7 demonstrates the potential distribution on the metal surface at the 81 hour mark at which pit propagation is occurring. Clearly, significant potential difference exists between anode and cathode with higher potential on the cathode and lower potential on the anode, as expected. As anode and cathode converge, they polarize each other making their electric potential increasingly alike. At the point where anode and cathode join together, a unique potential is experienced.

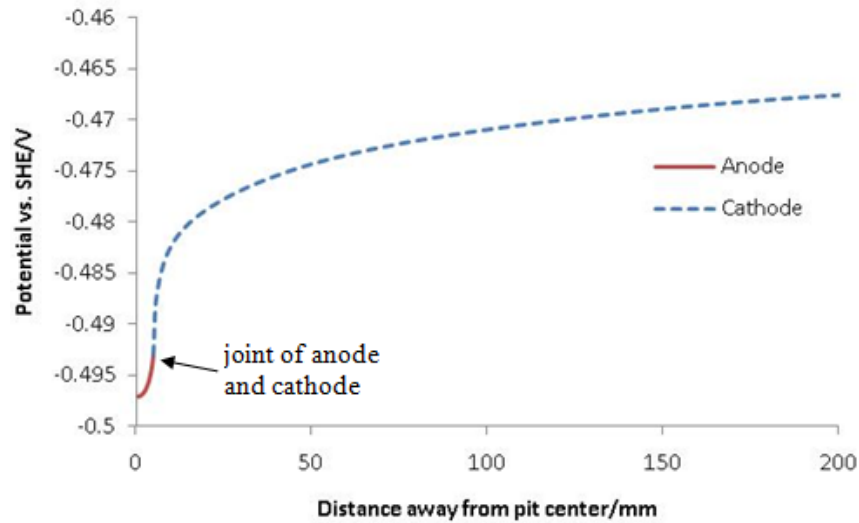


Figure 7: Potential distribution at metal surface at 81 hours. Simulation conditions: temperature 80°C, CO<sub>2</sub> partial pressure 0.52bar, velocity 0.4m/s, pipe diameter 0.1m, bulk pH 6.6, bulk supersaturation of FeCO<sub>3</sub> 1.05, passive current density 0.05A/m<sup>2</sup>.

Figure 8 shows the current density distribution along the metal surface at 81 hours. It can be seen that the current densities on the anode are much higher than those on the cathode. This is due to the fact that the current on the large area cathode must be balanced by a small area anode. Evidently, the metal surface is subject to a higher current density in the proximity of the interface between anode and cathode compared to the bulk anode and cathode surface. This is because in the area where anode and cathode are close to each other, the solution resistance decreases.

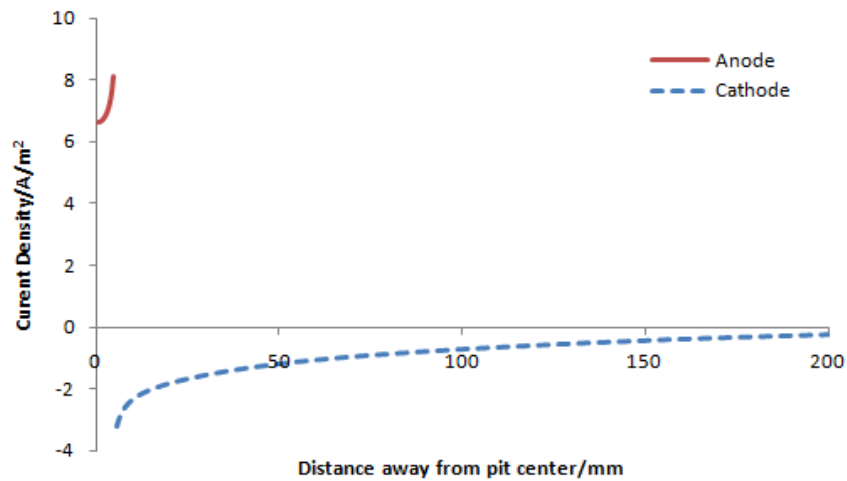


Figure 8: Current density distribution on steel surface at 81 hours. Positive current density stands for anode area while negative current density represents cathode area. Simulation conditions: temperature 80°C, CO<sub>2</sub> partial pressure 0.52bar, velocity 0.4m/s, pipe diameter 0.1m, bulk pH 6.6, bulk supersaturation of FeCO<sub>3</sub> 105, passive current density 0.05A/m<sup>2</sup>.

Figure 9 shows the effect of supersaturation of FeCO<sub>3</sub> [SS(FeCO<sub>3</sub>)] on corrosion rate. It can be seen that at bulk SS(FeCO<sub>3</sub>) of 12, occurrence of passivation is largely shifted to an earlier time compared to that for SS(FeCO<sub>3</sub>) of 1.05, as can be judged by the dramatic corrosion rate drop at about 57 and 68 hours, respectively. Whereas pit propagation was maintained at lower SS(FeCO<sub>3</sub>) of 1.05, repassivation takes place at this higher SS(FeCO<sub>3</sub>) of 12 due to the faster precipitation rate of FeCO<sub>3</sub>.

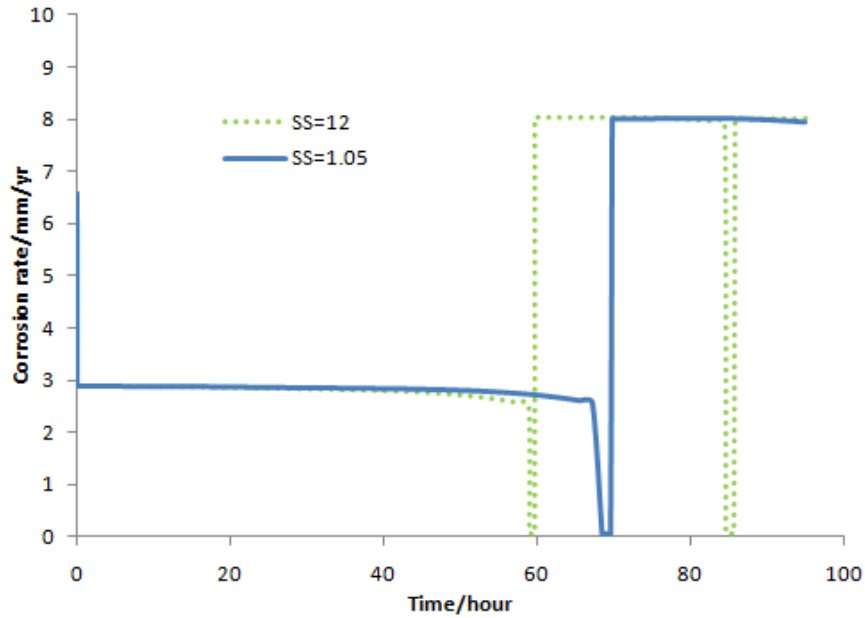


Figure 9: Corrosion rate comparison for bulk supersaturation with respect to  $\text{FeCO}_3$  at 1.05 and 12. Simulation conditions: temperature  $80^\circ\text{C}$ ,  $\text{CO}_2$  partial pressure 0.52bar, velocity 0.4m/s, pipe diameter 0.1m, bulk pH 6.6, passive current density  $0.05\text{A/m}^2$ .

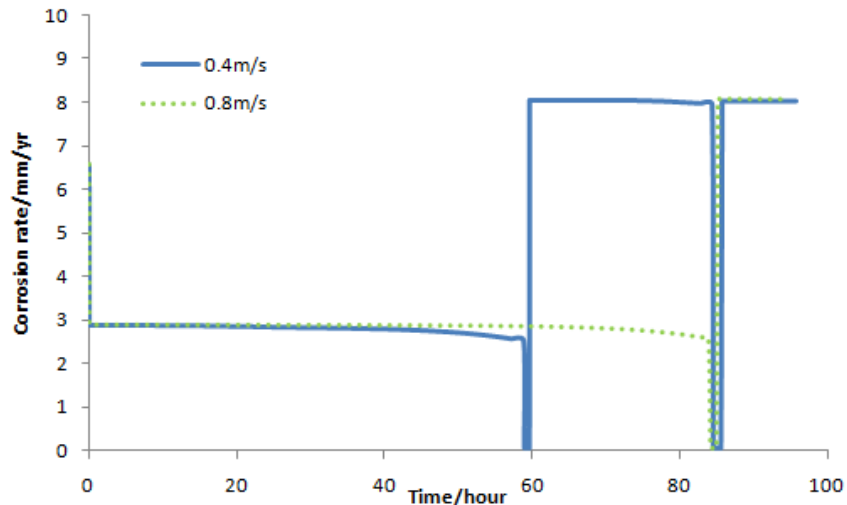


Figure 10: Corrosion rate comparison for bulk liquid velocity at 0.4m/s and 0.8m/s. Simulation conditions: temperature  $80^\circ\text{C}$ ,  $\text{CO}_2$  partial pressure 0.52bar, pipe diameter 0.1m, bulk pH 6.6, bulk supersaturation of  $\text{FeCO}_3$  12, passive current density  $0.05\text{A/m}^2$ .

Figure 10 compares the corrosion rate histories for two different liquid velocities at 0.4m/s and 0.8m/s, respectively. It can be seen that the higher liquid velocity postponed the occurrence of passivation as indicated by the sudden corrosion rate drop at about 84 hours. This is because higher bulk flow facilitates the transport process in which species, including  $\text{Fe}^{2+}$  and  $\text{CO}_3^{2-}$ , move towards or away from the metal surface at higher speeds, reducing the concentrations of  $\text{Fe}^{2+}$  and  $\text{CO}_3^{2-}$  and leading to a lower supersaturation of  $\text{FeCO}_3$  at the steel surface. As a result, the precipitation process proceeds much slower and inhibits the formation of  $\text{FeCO}_3$ . Due to an enhanced mass transport effect, pit propagation is maintained in higher liquid flow velocity, while repassivation is observed at a lower liquid velocity. It should be noted that in the case simulated, flow velocity does not appreciably affect the magnitude of

either uniform or localized corrosion rate. This is because that uniform corrosion rate is largely controlled by  $\text{CO}_2$  hydration rate and localized corrosion rate is attributed to the potential distribution which is mainly determined by the passive current density and solution conductivity.

Figure 11 and 12 show the measured galvanic current densities of carbon steel at different supersaturation with respect to  $\text{FeCO}_3$  in  $\text{CO}_2$  systems<sup>16</sup>. Clearly, pit propagation was observed for supersaturation 0.3~0.9, and pit death occurred when supersaturation increased to 3~9. This is consistent with the modeling results presented in this section.

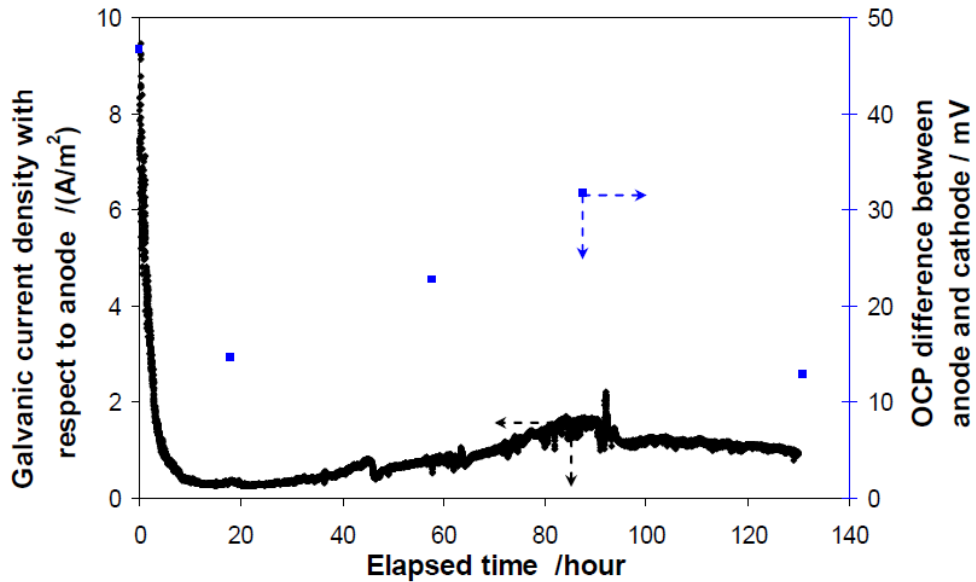


Figure 11 Galvanic current density and open circuit potential (OCP) difference between anode and cathode. Experiment conditions:  $\text{SSFeCO}_3=0.3-0.9$ ,  $T=80\text{ }^\circ\text{C}$ ,  $p\text{CO}_2=0.53\text{bar}$ ,  $\text{pH } 5.9-6.1$ ,  $[\text{NaCl}] = 1\text{ wt\%}$ , stagnant, shallow pit.<sup>16</sup>

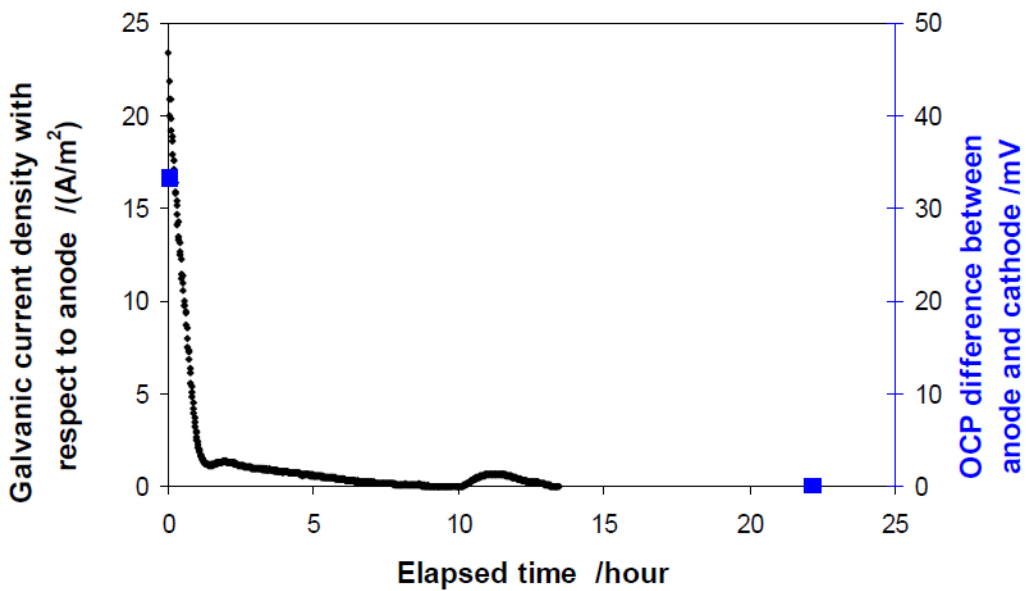


Figure 12 Galvanic current density and open circuit potential difference (OCP) between anode and cathode. Experiment conditions:  $\text{SSFeCO}_3= 3-9$ ,  $T=80\text{ }^\circ\text{C}$ ,  $p\text{CO}_2=0.53\text{bar}$ ,  $\text{pH } 5.6$ ,  $[\text{NaCl}] = 1\text{wt\%}$ , stagnant.<sup>16</sup>

## MODEL LIMITATIONS

The model presented in this paper was based on a series of fundamental laws which allows the exploration of closely related process parameters involved in corrosion, such as water chemistry and electrochemistry, in order to elucidate the mechanism(s) related to localized corrosion of carbon steel in a CO<sub>2</sub> environment. Calculated results have shown qualitative agreement with the general understanding of corrosion processes and experimental observations. However, like any other model, certain assumptions and limitations exist in the model.

Limitations of the current model are listed below:

- This model is a “2-point model” (a 1D simulation is done at two independent points: anode and cathode) for mass transport which is then coupled with a 2D model for potential/current distribution. Concentration gradients in the direction parallel to metal surface are assumed to be unimportant and are therefore neglected.
- An ideal solution is assumed, e.g., concentrations instead of activities are used for calculation, and species independently diffuse in the solution.
- The mechanism of pit initiation is arbitrary as the theory is still under development; proper kinetics of pit initiation is therefore not included.
- A constant value of passive current density is used in this model; this will be improved in the future by a mechanistically determined value.
- The effect of moving boundary seen with pit growth is neglected, which might become important at later stages of pit propagation.

A model calibration and validation process is under way with the aim of making the model suitable for practical use.

## CONCLUSIONS

- A mechanistic model has been developed for prediction of corrosion processes (including localized corrosion) of carbon steel in CO<sub>2</sub> environment. A series of fundamental laws are used to construct the model in order to generate reasonable results.
- Pit propagation is closely related to surface water chemistry and surface electrochemistry. Pit propagation rate is driven by potential difference between anode and cathode and limited by solution resistance.
- The model shows no pit acidification occurring inside the pit of carbon steel in CO<sub>2</sub> environment due to strong buffering effect of the CO<sub>2</sub> solution.
- The model suggests that lower supersaturation with respect to FeCO<sub>3</sub> and higher liquid flow tend to maintain pit propagation, while higher saturation and low liquid flow facilitates repassivation.

## ACKNOWLEDGEMENTS

The authors would like to acknowledge the technical guidance and financial support provided by the sponsor companies of the Corrosion Center Joint Industry Project at Ohio University. They are Baker Petrolite, BG Group, BP, Champion Technologies, Chevron, Clariant Oil Services, ConocoPhillips, Encana, ENI S.p.A., ExxonMobil, WGIM, Total, NALCO Energy Services, Occidental Petroleum Co., Petrobras, PETRONAS, PTT, Saudi Aramco, Teikoku Oil.

## REFERENCES

1. M. Nordsveen, S. Netic, and A. Stangeland, "A Mechanistic Model for Carbon Dioxide Corrosion of Mild Steel in the Presence of Protective Iron Carbonate Films—Part 1: Theory and Verification," *Corrosion* 59, 5(2003), pp:443-456.
2. S.M.Sharland, "A Review of the Theoretical Modeling of Crevice and Pitting Corrosion", *Corrosion Science* 27,3(1987), pp:289-323.
3. J. Han, D.Young, H.Colijn, A. Tripathi and S. Netic, Chemistry and Structure of the Passive Film on Mild Steel in CO<sub>2</sub> Corrosion Environments. *Industrial & Engineering Chemistry Research*, 2009. 48(13): pp. 6296-6302.
4. J. Han, Y. Yang, B. Brown, S. Netic, "Roles of Passivation and Galvanic Effects in Localized CO<sub>2</sub> Corrosion of Mild Steel," *CORROSION/2008*, Paper no. 332 (Houston, TX: NACE, 2008).
5. E. Eriksrud, T. Sontvedt, "Effect of Flow on CO<sub>2</sub> Corrosion Rates in Real and Synthetic Formation Waters" , in *Advances in CO<sub>2</sub> Corrosion* ,Vol.1. Proc. Corrosion/83 Symp. CO<sub>2</sub> Corrosion in the Oil and Gas Industry, eds. R.H.Hausler, H.P.Goddard (Houston, TX:NACE,1984), pp:20.
6. S. Netic, H. Li, J. Huang and D. Sormaz, "A Free Open Source Mechanistic Model for CO<sub>2</sub> / H<sub>2</sub>S Corrosion of Carbon Steel", *CORROSION/2009*, Paper no. 572 (Houston, TX: NACE, 2009).
7. S. Netic, J. Postlethwaite, and S. Olsen, An Electrochemical Model for Prediction of Corrosion of Mild Steel in Aqueous Carbon Dioxide Solutions. *Corrosion*, 1996. 52(4): p. 280-294.
8. J. R. Vera, D. Shirah, F. Song, Laboratory Evaluation of Galvanic CO<sub>2</sub> Corrosion and Inhibition of Carbon Steel Piping Partially Clad With Alloy 625, *NACE/2009*, Paper no. 566 (Houston, TX: NACE, 2009).
9. H. Ascher, "Repairable Systems Reliability— Modeling, Inference, Misconceptions and Their Causes", Marcel Dekker, New York(1984).
10. DNV RP G101, "Risk Based Inspection of Offshore Topsides Static Mechanical Equipment", DET NORSK VERITAS, Norway (January 2002).
11. H. W. Pickering, "Important Early Developments and Current Understanding of the IR Mechanism of Localized Corrosion", *Journal of Electrochemical Society* 150, 5(2003), pp: K1-K13.
12. J.S. Newman, "Electrochemical Systems", 2nd edition, Englewood Cliffs, NJ, Prince Hall (1991).

13. . J. T. Davies, “Turbulence Phenomena”, London, U.K., Academic Press.(1972).
14. S. Netic and K.-L.J. Lee, “A Mechanistic Model for Carbon Dioxide Corrosion of Mild Steel in the Presence of Protective Iron Carbonate Films—Part 3: Film Growth Model”, Corrosion 59, 7 (2003), pp:616-627.
15. K. Heppner, “Development of Predictive Models of Flow Induced and Localized Corrosion,” Ph.D. Thesis, University of Saskatchewan (May 2006).
16. J. Han, “Galvanic Mechanism of Localized Corrosion for Mild Steel in Carbon Dioxide Environments”, Ph.D. Thesis, Ohio University (November 2009).